Eur. Phys. J. B **16**, 337–344 (2000)

THE EUROPEAN PHYSICAL JOURNAL B

EDP Sciences

Competition between kinetic and surface tension anisotropy in dendritic growth

T. Ihle[a]

Minnesota Supercomputer Institute, University of Minnesota, 1200 Washington Ave. South, Minneapolis, MN 55415, USA

Received 30 September 1999 and Received in final form 23 February 2000

Abstract. The combined effect of an anisotropic surface tension and interface kinetics in dendritic crystal growth is studied numerically by a fully dynamical front-tracking method in two dimensions. It is shown how kinetic effects can be incorporated into the algorithm without causing numerical instabilities. The results are compared to the theory of E.A. Brener and V.I. Mel'nikov (Adv. Phys. **40**, 53 (1991)). A particularly interesting case arises when the directions of minimum surface tension and minimum kinetic effect are different. In this case, when the deviation from local equilibrium is increased, the predicted transition from dendrites growing into the direction of the minimum surface stiffness to the direction of minimum kinetic effect is confirmed. Dendrites near this transition show strong oscillations and correlated side-branching. The transition where the oscillating dendrites change direction shows hysteresis.

PACS. 81.10.Aj Theory and models of crystal growth; physics of crystal growth, crystal morphology and orientation – 68.70.+w Whiskers and dendrites (growth, structure, and non-electronic properties) – 05.70.Fh Phase transitions: general studies

1 Introduction

Diffusion-controlled growth is a typical example of pattern formation in nonequilibrium systems [1]. It occurs when two possible phases of a system are driven out of coexistence so that one of the phases grows at the expense of the other phase. This type of phase change usually requires the diffusive transport of at least one conserved quantity such as the latent heat of solidification. It is assumed here that the two phases do not mix perfectly but are separated by an interface which moves during the growth. The dynamics and shape of this moving boundary can be very complicated and requires an efficient numerical algorithm. Recently, a front-tracking method was developed in which the interface is treated explicitly and coupled to a diffusion field which is discretized on a cubic lattice [2]. The artificial anisotropy introduced by the lattice is significantly reduced by averaging over a stack of lattices which are rotated with respect to each other. The algorithm does not rely on the quasi-stationary approximation and has been successfully applied to study non-stationary problems with a complex and even fractal shape of the interface [3].

Originally, the method was designed to treat solidification under the assumption of local thermal equilibrium at the solid-liquid boundary. However, this is only realized when the interface kinetics is infinitely fast. Usually, for the interface to grow, a finite driving force such as undercooling is required at the interface. Above the roughening temperature, and for small deviations from equilibrium, there is an Onsager relation between the driving force and the response of the interface: the growth velocity of the interface is equal to the interface undercooling times a kinetic coefficient. This effect is of particular importance in directional solidification of certain organic crystals [4], and in step-flow growth of metals and semiconductors during Molecular Beam Epitaxy [5], which can be described by the Burton-Carbrera-Frank model [6].

The most frequently encountered growth morphology in diffusion-controlled growth is the dendrite. The dendritic shape is basically a "needle crystal" with a parabolic tip decorated on its sides by secondary branches. It has been shown that the anisotropy of the surface tension plays an essential role in the selection of the shape and the growth speed of the dendrite [7–9]. In fact, no dendrites are possible in isotropic systems. The crystalline anisotropy considered here is assumed to be sufficiently small and nonsingular so that the crystal will not exhibit facets. It is less well-known that the selection of dendrites can also be determined exclusively by the anisotropy of the kinetic coefficient [10]. In this paper, I show how kinetic effects can be incorporated into the algorithm without causing numerical instabilities. This method is used to investigate the combined effect of interface tension and interface kinetics on the growth of dendrites. The kinetic effect is expected to determine the selection at large driving forces. At small undercooling the dendrite operating point should be dominated by the surface tension anisotropy. The situation where the direction of minimum surface

[a] e-mail: ihle@msi.umn.edu

stiffness agrees with the direction of minimum kinetic effect has been studied numerically by Saito *et al.* [11] with a quasistationary Green's function approach. When those directions differ, an oscillatory instability has been predicted [12] which cannot be treated with this approach, but requires a fully-dynamical method.

The system considered here is a two-dimensional crystal growing into its undercooled melt in which the growth is controlled by the diffusion of the latent heat of freezing. Deep in the liquid, the temperature T_∞ is kept below the melting temperature T_M. Due to the latent heat L (per unit volume) produced by solidification, the temperature T near the solid is elevated. The normalized temperature field, $u = c_p(T - T_\infty)/L$, obeys the diffusion equation,

$$\frac{\partial u}{\partial t} = D\nabla^2 u\,, \tag{1}$$

where D is the thermal diffusivity and c_p the specific heat. When the crystal is growing with a normal velocity v_n, the latent heat produced at the solidification front is transported away by the heat flow. Conservation of energy then implies

$$v_\mathrm{n} = -D\,\nabla u \cdot \mathbf{n}\,, \tag{2}$$

where $\mathbf{n}$ is the normal vector of the interface. For simplicity, only the so-called one-sided model is considered here in which diffusion takes place only on the "liquid" side of the interface. A generalization to a two-sided model is straightforward and necessary for other applications such as the growth of vicinal surfaces [5,13]. A rough non-faceted interface can be regarded as being in local equilibrium, and the temperature of a planar interface is equal to the melting temperature T_M. For a curved interface with local curvature κ, the equilibrium value of u_eq is reduced by the Gibbs-Thomson effect according to

$$u_\mathrm{eq} = \Delta - d\kappa\,, \tag{3}$$

where $\Delta = c_p(T_\mathrm{M} - T_\infty)/L$ is the dimensionless undercooling and d is an anisotropic capillary length obtained from an orientation-dependent interfacial tension $\gamma(\theta)$ as

$$d(\theta) = \left(\gamma + \frac{\partial^2\gamma}{\partial\theta^2}\right)\frac{T_\mathrm{M}c_p}{L^2}\ . \tag{4}$$

For a crystal to grow, the interface must be undercooled so that the temperature at the interface, u_i, differs from u_eq. This temperature difference acts as a driving force and is linearly related to the heat flux *via* the Onsager-relation

$$u_\mathrm{i} - u_\mathrm{eq} = \beta(\theta)\ \ [D\,\nabla u \cdot \mathbf{n}]\ , \tag{5}$$

where $\beta(\theta)$ is an anisotropic kinetic coefficient. It follows that the normalized temperature field at the interface, u_i, must fulfill the boundary condition

$$u_\mathrm{i} = \Delta - d\kappa - \beta v_\mathrm{n}\,. \tag{6}$$

In the following, the crystal is assumed to have a cubic symmetry, so that both the capillary length and the kinetic coefficient have a fourfold symmetry

$$d(\theta) = d_0(1 - \varepsilon_\mathrm{S}\cos 4\theta)\,, \tag{7}$$

$$\beta(\theta) = \beta_0(1 - \varepsilon_\mathrm{K}\cos[4(\theta - \theta_0)])\,, \tag{8}$$

where ε_S and ε_K are small parameters which characterize the anisotropy of the surface stiffness and of the kinetic effect, respectively. The directions of minimum capillary length (or minimum surface stiffness) and minimum kinetic effect are not necessarily the same. For the assumed cubic symmetry these two directions can differ by an angle $\theta_0 = \pi/4$. In the absence of surface tension and kinetic effects, *i.e.* $d_0 = 0$, and $\beta_0 = 0$, Ivantsov [14] showed that a parabolic needle crystal will grow steadily with a tip radius ρ. The undercooling Δ determines the product of tip radius and the growth velocity v, or the Peclet number $p = v\rho/(2D)$, by the relation

$$\Delta = 2\sqrt{p}\,\mathrm{e}^p \int_{\sqrt{p}}^{\infty} \exp(-x^2)\,\mathrm{d}x \tag{9}$$

in two dimensions. However, the growth mode cannot be determined uniquely since there are an infinite number of possible combinations of v and ρ for a given product p. Furthermore, all Ivantsov parabolas were found to be unstable against small perturbations. The solvability theory for infinitely fast kinetics ($\beta_0 = 0$) [7–10] showed that interface tension together with a non-zero anisotropy ε_S is necessary to stabilize a unique Ivantsov-parabola against infinitesimal perturbations. The universal scaling law $vd_0/(2Dp^2) = \sigma(\varepsilon_\mathrm{S})$ for the growth rate was derived, which shows that σ depends only on the anisotropy ε_S of the capillary length, but is independent of the undercooling Δ. This scaling relation has been confirmed by previous numerical simulations [15,16]. For small anisotropy, σ was shown to be proportional to $\varepsilon_\mathrm{S}^{7/4}$, and the velocity scales as

$$v \sim \varepsilon_\mathrm{S}^{7/4}\frac{Dp^2}{d_0}\ . \tag{10}$$

2 Numerical method

The diffusion equation (1) together with the boundary conditions (2) and (3) can be solved using a finite difference approach, in which the temperature field is discretized on a simple (cubic) grid. The interface is represented by a set of points (interface points) which are thought to be connected with straight lines, and the boundary conditions on them are interpolated from the nearest-neighbor points. The distance between interface points changes during the growth, but is kept approximately constant by inserting and removing points. The positions of interface points are not restricted to grid points of the diffusional lattice. This requires extrapolation and interpolation procedures to establish the right boundary conditions for the temperature field and to calculate

the normal velocity of every interface point by means of equation (2).

Every interface point is shifted by $v_{\rm n}\,\delta t\,\mathbf{n}$ during an iteration with the time step δt. The grid introduces a significant amount of artificial anisotropy because it is not adapted to the shape of the interface. This error can be greatly reduced by solving the diffusion equation simultaneously on several grids (typically two or four) which are rotated with respect to each other. In every timestep, the interface points are advanced with velocities which are averaged over those grids (see [2] for details). A naive way to incorporate kinetics into this method is to modify the Gibbs-Thomson boundary condition by the kinetic coefficient (Eq. (6)) and to use the normal velocity determined in the previous time step. This works well for small kinetic coefficients $\beta_0 < 0.5$, and a stationary dendritic solution was found. Unfortunately, at large deviations from local equilibrium, $\beta_0 > 0.5$, an oscillatory numerical instability occurred: already after 5 to 10 time steps the values of the local velocities at almost all interface points increased without bound and the sign of the velocities alternated during the iterations. This rapid evolution of the instability led to the assumption that the dynamics of the diffusion field is irrelevant here, and that the instability is caused by an inconsistent implementation of the boundary condition (6). On the one hand, condition (6) is used in the procedure to calculate the local velocity by means of the gradient of the diffusion field. On the other, the condition depends itself on the local velocity. I show below that it is indeed this feed-back mechanism which causes the numerical oscillatory instability.

The calculation of the normal velocity and the determination of the boundary condition can be approximately described by

$$v^m = \frac{D}{a}(u^m - \tilde{u}) \tag{11}$$

$$u^{m+1} = \Delta - \beta v^m, \tag{12}$$

where a is the lattice constant of the diffusional grid, and m denotes the number of iterations. Curvature effects are neglected here for simplicity, and $\tilde{u}$ is the value of the diffusion field in the "liquid" phase, a distance a from the interface. Equation (11) is a very simplified implementation of (2) and describes the basic features of how the gradient of the diffusion field at the interface points is determined in the front-tracking algorithm (see [2] for details of the method). $\tilde{u}$ is determined by interpolation from the surrounding nodes of the diffusional lattice. In this analysis $\tilde{u}$ is assumed to be time-independent on the fast time scale of the instability. This decoupling from the dynamics of the diffusion field makes it possible to close the set of equations, (11, 12), and to solve them easily. Inserting (11) into (12) yields

$$u^{m+1} = \Delta - \frac{\beta D}{a}(u^m - \tilde{u}). \tag{13}$$

Define the stationary solution $u_{\rm s}$ of this equation by $u_{\rm s}^{m+1} = u_{\rm s}^m$, and express u^m as $u^m = u_{\rm s} + \delta u^m$. The solution for δu^m can be easily found to be

$$\delta u^m = \left(-\frac{\beta D}{a}\right)^m \delta u^0\,. \tag{14}$$

Hence, the stationary solution is only stable, *i.e.* $\delta u^m \to 0$ for $m \to \infty$, when $\beta D/a < 1$. The critical kinetic coefficient $\beta_{\rm C} = 1$ ($D = 1$ and $a = 1$ in the simulation) is of the same order of magnitude than the value $\beta_{\rm C} \approx 0.5$ found numerically.

One possibility to avoid this instability would be to use an implicit method, in which the boundary value $u_{\rm i}$ is determined self-consistently. However, this is very time-consuming because the actual formula to determine the local velocity is much more complex than equation (11) and is coupled to the neighboring interface points. Therefore, a simple adaptive method is used which is much more efficient, at the cost of small numerical errors which can be reduced by using smaller time increments δt. The idea is to use another velocity $\tilde{v}_{\rm n}$ instead of $v_{\rm n}$ in the boundary value equation (6). This velocity is constructed to change slowly, but to converge to $v_{\rm n}$ (for simplicity the index n for the normal direction is omitted in the following):

$$\tilde{v}^m = \tilde{v}^{m-1} - \frac{1}{\tau}(\tilde{v}^{m-1} - v^m)\,. \tag{15}$$

By going to the limit $\tau \to \infty$ it can be easily seen that this method should be able to eliminate the instability. In this case, $\tilde{v}$ is a constant and the actual velocity $v_{\rm n}$ does not appear at all in the boundary condition. This corresponds to the situation of local equilibrium (with a renormalized undercooling $\tilde{\Delta} = \Delta - \beta\tilde{v}$), which is stable. Of course, in the actual simulation, the time scale τ has to be small compared to the time scale of the structure formation. Otherwise, the actual dynamics of the pattern, such as the formation of bumps, oscillations of the dendritic tip, etc., would depend on the artificial dynamics of $\tilde{v}$. This separation of time scales can be easily achieved, because the instability depends only on the number of iterations m, but not on the physical time step δt. That means going to very small time steps makes the dynamics of the pattern formation very slow compared to τ.

Let us analyse how large τ should be to suppress the instability. equation (12) is modified to

$$u^{m+1} = \Delta - \beta\tilde{v}^m\,, \tag{16}$$

where $\tilde{v}^m$ is given by equation (15). Successive insertion of (11) and (15) for m, $m-1$, $m-2$, ... into equation (16) yields

$$u^{m+1} = \Delta - \frac{\beta D}{a\tau}\sum_{l=0}^{m-1}\left(1-\frac{1}{\tau}\right)^l \{u^{m-l} - \tilde{u}\} - \beta\left(1-\frac{1}{\tau}\right)^m \tilde{v}^0\,. \tag{17}$$

For large m and $\tau > 0.5$, the last term can be neglected, and the stationary solution is obtained as

$$u_{\rm s} = \Delta - \frac{\beta D}{a\tau}(u_{\rm s} - \tilde{u})\sum_{l=0}^{m-1}\left(1-\frac{1}{\tau}\right)^l\,. \tag{18}$$

For $m \to \infty$, it follows that $u_s = \Delta - \beta D(u_s - \tilde{u})/a$, as expected, because the relaxation procedure (15) must not influence the stationary solution. For a small perturbation, δu, of the stationary solution one has

$$\delta u^{m+1} = K\left(\delta u^m + R\delta u^{m-1} + R^2\delta u^{m-2} + ...\right) , \quad (19)$$

with $K = -\beta D/(a\tau)$, and $R = 1 - 1/\tau$. Assuming δu^m to be zero for all $m < 0$, an iterative solution of (19) yields

$$\delta u^{m+1} = K(K+R)^m \, \delta u^0 . \quad (20)$$

Stability is achieved if $|K + R| < 1$, *i.e.* if

$$\tau > \frac{1}{2}\left(1 + \frac{D\beta}{a}\right) . \quad (21)$$

This provides a stable iteration scheme for the self-consistent determination of the boundary condition during the evolution of the interface. By choosing a sufficiently large relaxation time τ, the algorithm remains stable even for large kinetic coefficients β_0. After implementing this scheme, the observed numerical instabilities at large β_0 disappeared. The necessary minimum τ was slightly larger than given in condition (21). This is not surprising since the present analysis is strongly simplified and neglects the curvature of the interface as well as the relaxation of the diffusion field. As described later, oscillating dendrites were found for certain values of the growth parameters. In order to check whether these oscillations are influenced by the stabilization dynamics, τ was increased by a factor of two. No significant change of the oscillations were found, which proves that the relaxation scheme can also be used to study non-stationary structures.

3 Results and conclusion

First, the case without competition of the kinetic effects and the surface tension is considered, *i.e.*, where the angle θ_0 defined in (8) is zero. The numerical code was checked by comparing results with previous simulations of dendrites using a Green's function method [11]. Especially significant is a comparison at large kinetic coefficients, *i.e.*, in a growth regime dominated by the kinetic effect. For this purpose, calculations were performed at undercooling $\Delta = 0.45$ and a ratio $\nu = \varepsilon_K/\varepsilon_S = 1$ (see columns 1 and 2 in Tab. 1). The preferred directions of the two anisotropies are the same, *i.e.* $\theta_0 = 0$. The values for the growth velocities agree very well (within 9%), whereas the measured tip radii are slightly too large. This discrepancy is not dramatic, since the values for the radii are very small in internal units, around 2 to 4 lattice units of the diffusional grid, which is very close to the limit of numerical resolution.

Next, simulations were performed in the purely kinetic growth regime, $p\sqrt{\varepsilon_K}D\beta_0/d_0 \gg 1$, where the selection of dendrites is supposed to be independent of the capillary length d_0 and the diffusion constant D. Brener *et al.* [10] predicted the growth rate to be

$$v = \frac{p\varepsilon_K^{5/4}}{\gamma_0\beta_0} , \quad (22)$$

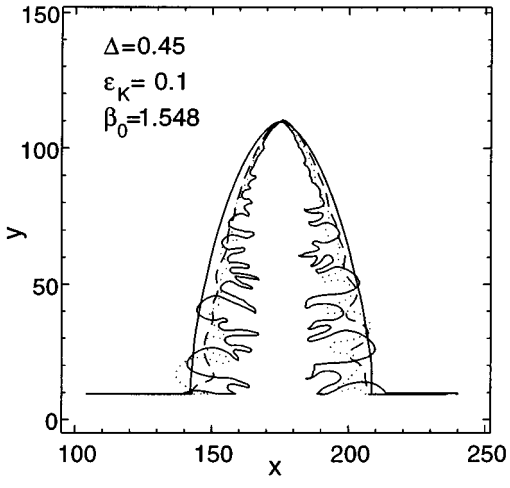

Fig. 1. Kinetic dendrite with isotropic surface tension, $\varepsilon_S = 0$, for decreasing capillary length: $d_0 = 0.031$ (smooth solid line), $d_0 = 0.0155$ (dashed), $d_0 = 0.0077$ (dotted), and $d_0 = 0.0008$ (solid line with many side-branches). See also column 3 to 6 in Table 1. Parameters: $\Delta = 0.45$, $\varepsilon_K = 0.1$, $\beta_0 = 1.5485$, $D = 1$. Here and in the following, all length scales are given in internal units of the diffusional grid δx, and all time scales are given in units of $\delta x^2/D$.

where γ_0 is a constant of order one. p is the Peclet number which is related to the undercooling Δ by equation (9). Four calculations were performed (columns 3 to 6 in Tab. 1), in which d_0 was successively reduced. It was found that the growth velocity v was not inversely proportional to d_0, as for a dendrite without kinetic effect, (10), but changed less and less with decreasing d_0. The extrapolation of the data to $d_0 = 0$ resulted in a very small value for the constant $\gamma_0 = 0.0877$. The growth at $d_0 = 0$ could not be directly simulated. For small d_0 the dendritic tip remained stable, but the interface became rougher and rougher as d_0 was decreased, because the distance between side-branches scales with d_0 (see Fig. 1).

There is a more interesting situation, where the preferred directions of the anisotropic kinetic coefficient and the capillary length are different. In two dimensions, and with the cubic symmetry considered here, the only possible angle between these two directions is $\theta_0 = \pi/4$. In this case both effects are competing. The theory of Brener *et al.* discusses all possible patterns in terms of the two parameters:

$$\mu = 2p\varepsilon_S^{1/2}\frac{D\beta}{d_0} ,$$

and

$$\nu = \frac{\varepsilon_K}{\varepsilon_S} . \quad (23)$$

μ measures the strength of the kinetic effect compared to the effect of the surface tension, and ν is the ratio of the two anisotropies. For all values of μ, stationary dendrites are predicted which grow into the direction of the capillary length (capillary dendrites). There is another branch

Table 1. Simulation of kinetic dendrites on two rotated grids. Parameters: undercooling $\Delta = 0.45$, time step $\delta t = 0.47$, mesh size 371×371, channel width $L = 230$, relaxation time $\tau = 6.4$ for artificial boundary dynamics. Symbols: ε_S: fourfold anisotropy of the capillary length, ε_K: fourfold anisotropy of the kinetic coefficient, d_0: capillary length, β_0: kinetic coefficient, V_{Tip}: stationary growth velocity of the dendrite, R_{Tip}: radius of curvature at the tip of the dendrite, P_{geo}: geometrical peclet number $P_{geo} = V_{Tip}R_{Tip}/(2D)$. The values in parentheses were taken from [11] for comparison. All length scales are given in units of the diffusional grid δx, and all time scales are given in units of $\delta x^2/D$.

Run	1	2	3	4	5	6
ε_S	0.1	0.1	0	0	0	0
ε_K	0.1	0.1	0.1	0.1	0.1	0.1
d_0	0.03097(0.001)	0.0144(0.001)	0.03097	0.0155	0.0077	0.0008
β_0	1.5485(0.05)	2.1662(0.15)	1.5485	1.5485	1.5485	1.5485
V_{Tip}	0.0347(0.034)	0.0369(0.034)	0.0317	0.0435	0.050	0.058
R_{Tip}	3.4(2.911)	2.45(1.566)	3.98	2.57	2.2±0.2	1.85±0.3
P_{geo}	0.059(0.0495)	0.0452(0.02664)	0.0631	0.0559	0.0550	0.0536

of solutions – dendrites growing into the direction of minimum kinetic effect (kinetic dendrites), *i.e*, at an angle of $\pi/4$ with respect to the capillary dendrites. However, this is only possible above a certain critical value μ_{crit}. At these high values of μ the capillary dendrites should grow slower than the kinetic ones and are very likely to be linearly unstable. According to theory, no other growth directions are possible. This is fully consistent with the behavior shown in Figure 2b: Far above μ_{crit} a dendrite growing into the "wrong" direction of the minimum capillary length was initialized. This solution turned out to be unstable: two kinetic dendrites growing at an angle of $\pi/4$ with respect to the initial direction developed from the first side-branches of the original crystal.

A linear stability analysis in the framework of the Boundary-Layer Model [17] by Liu *et al.* [12] showed that for increasing μ, capillary dendrites become unstable even before kinetic dendrites exist. They found a gap, $\mu_1 < \mu < \mu_2$, $\mu_2 \gtrsim \mu_{crit}$, in which both types of dendrites show an oscillatory linear instability and observed complex non-stationary patterns. This excluded the possibility of a coexistence of both types of dendrites. So far, this transition has not been investigated within the exact fully-dynamical solidification model. The critical value μ_{crit} depends on ν, and is supposed to be of the order of one at $\nu = 1$. Elsewhere one has

$$\begin{aligned} \mu_{crit} &\sim \nu^{-1} \qquad \text{for } \nu \gg 1 \\ \mu_{crit} &\sim \nu^{-3/2} \qquad \text{for } \nu \ll 1\,. \end{aligned} \tag{24}$$

To investigate the transition at $\nu = 1$, a dendrite was initialized with $\mu = 4.28$ in a broad channel with reflecting boundary conditions. The direction of the channel was chosen to be the same as the expected growth direction of a kinetic dendrite. Since $\mu \gg 1$, the initialized needle crystal relaxes towards a kinetic dendrite without changing the direction of growth. Figure 2a shows the final state superimposed with a picture of a dendrite where the angle θ_0 between the two anisotropies is zero. We note that there is only a slight difference in the shape of the structure, which in an experiment would make it hard to tell which one of the two cases $\theta_0 = 0$ or $\theta_0 = \pi/4$ is realized.

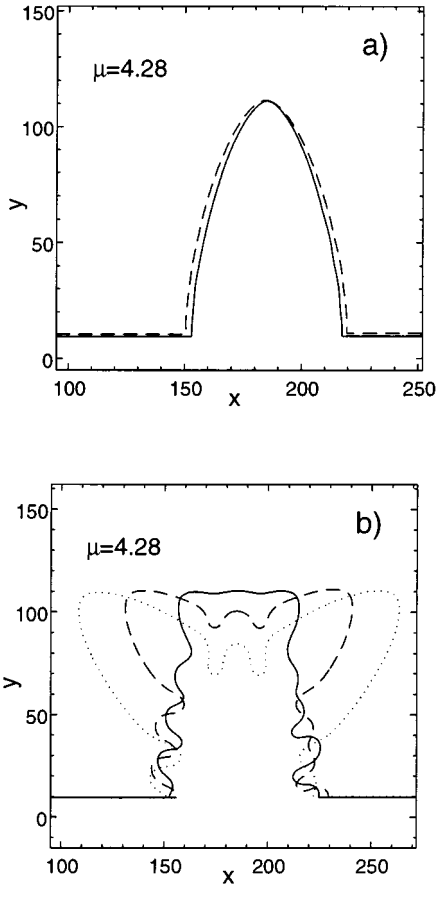

Fig. 2. (a) The final state of a kinetic dendrite at $\mu = 4.28$ and $\theta_0 = \pi/4$ (dashed line). Superimposed is a dendrite with the same parameters, but $\theta_0 = 0$ (solid line). The direction of growth is determined by the minimum of the kinetic effect. (b) Snapshots of the initial development of a dendrite $\mu = 4.28$ and $\theta_0 = \pi/4$ which was initialized in the "wrong" direction, *i.e.* the direction of minimum capillary length and maximum kinetic effect. This structure is not stable and the first side-branches develop into two kinetic denrites growing at an angle of $\pi/4$ with respect to the axis of the channel. Parameters: $d_0 = 0.031$, $\Delta = 0.45$, $\beta_0 = 1.5485$, $D = 1$, $\varepsilon_S = \varepsilon_K = 0.1$.

The transition area $\mu \sim 1$ was approached from above by successively reducing μ. In all following simulations μ was changed only by changing the kinetic coefficient β_0; all other growth parameters were kept constant. After every change of μ, the calculation was continued until the pattern had reached a new stationary state. Near $\mu \sim 1$, strong oscillations of the tip radius and the velocity were observed. Although the dendritic tip was no longer parabolic, but periodically deformed by strong sidebranching, the basic structure of a dendrite survived: one main shaft decorated with branches. The structure of the side-branches and the oscillations are very regular because both sides of the shaft are synchronized and communicate through the deformation of the tip. I call this structure an oscillating kinetic dendrite, because its appearance is still very close to that of an ordinary dendrite.

For smaller μ, two oscillating capillary dendrites were born growing at an angle of $\pi/4$ with respect to the axis of the channel. Of course, this setup cannot be used to further investigate these dendrites since they would soon hit the wall of the channel. Therefore, I investigated the transition starting with a capillary dendrite at small $\mu \ll 0.5$ growing parallel to the axis of the channel. The temporal evolution of this dendrite at $\mu = 0.25$ is shown in Figure 3a. Basically, the scenario for increasing μ looks the same as that observed for the kinetic dendrites for decreasing μ: the formation of side-branches becomes stronger and stronger, which causes strong oscillations of the velocity with periodic asymmetric deformations of the tip. This is shown for $\mu = 0.4$ and $\mu = 0.6$ in Figures 3b and 3c, respectively. Compared to Figure 3a, the side-branches are much larger and more regular. The corresponding velocities and tip radii are plotted as a function of time in Figure 4. The period of the oscillations agrees within 30% with the convective time scale $T_{\mathrm{con}} = V_{\mathrm{Tip}}/\Lambda$, where Λ is the distance between side-branches. At sufficiently large μ, the average growth direction changed and a kinetic dendrite started to grow at an angle of $\pi/4$ with respect to the previous direction.

Two fundamental mechanisms for the formation of sidebranches have been discussed in the literature: (i) a non-linear mode of tip-splitting or dynamical tip oscillations, and (ii) the selective amplification of thermal noise. The latter mechanism consists of a convective instability triggered at the tip of the dendrite by the surrounding noise. Noise-induced wavepackets generated in the tip region grow exponentially in amplitude, and spread and stretch as they move down the sides of the dendrite, producing a train of sidebranches. This instability is analogous to the so-called Mullins-Sekerka instability of a planar front, translated to a parabolic front.

Recently, the linear theory of noise-amplification [18] has been improved substantially by Brener *et al.* [19]. They showed that the amplification rate depends very sensitively on the shape of the crystal. Experiments for the sidebranching of xenon dendrites [20], as well as phase-field simulations with included noise [21], are in quantitative agreement with this theory.

In the other proposed mechanism for sidebranching, (i), it is argued that nonlinearities in the equation of motion can lead to a stable oscillating growth mode [22] which can act as a source of the sidebranches. Tip oscillations lead to a more or less periodic appearance of the branches and to a correlation between sidebranches on opposite sides of the dendrite. Although no tip oscillations were detected in the free growth experiment mentioned above, which excludes mechanism (i), it seems to apply to other systems. The experiments of Georgelin *et al.* [23] for directional solidification were only in part consistent with the theory of noise-amplification. They observed strong correlations of the sidebranches on opposite sides of the dendrites for certain parameters, consistent with a phase locking growth mechanism. This is exactly what is found here near the transition point between the kinetic and the capillary dendrite. Far from the transition we have the ordinary noise-amplification mechanism (ii) of free growth, but close to the transition the non-linear mechanism (i) was observed: Sidebranches themselves induce perturbations to which the tip, where new sidebranches are generated, is sensitive. This feature results from a competition between the direct effect of the noise and the non-linear effect of the feedback. The noise in my simulations is non-thermal. It originates from the small intrapolation and extrapolation errors of the front-tracking algorithm.

This feedback mechanism has been observed earlier as a transient in simulations of free dendritic growth at low anisotropy and large (non-thermal) noise [2]. In this situation sidebranches grow very quickly and are not convected fast enough away from the tip to leave the tip unperturbed. They cause an asymmetric, periodic deformation of the tip and oscillations of the tip velocity. This was not observed in recent simulations by the phase-field model [21], probably because the noise level was lower and an artificial symmetry of the dendrite was imposed which prevents asymmetric tip-deformations.

The correlation of sidebranches on both sides of the dendrite in free growth can also be achieved by external means, such as periodic heating or pressure changing [24], heating of the dendrite tip by a laser beam [25], or imposing an oscillatory flow field [26]. Sidebranches coupled to an oscillating tip have also been found numerically in narrow channels with a mismatch between the orientation of the channel and the direction of minimum surface stiffness [27].

In Figure 5 the growth rate of the dendrites (normalized and averaged over time) in the stationary state is plotted as a function of μ. The growth rate of both branches of the solution reaches a minimum near the transition point. μ_{crit} is defined as the value where the velocity of both branches is the same: $\mu_{\mathrm{crit}} = 0.617$. The interesting feature of this transition is that there is hysteresis on both sides of μ_{crit}, *i.e.*, the transition is of first order. For μ slightly smaller than μ_{crit}, both types of oscillating dendrites are stable, with the capillary structure growing faster than the one controlled by the kinetic effect. For μ slightly larger than μ_{crit}, both types of oscillating dendrites are still stable, but now the capillary structure is

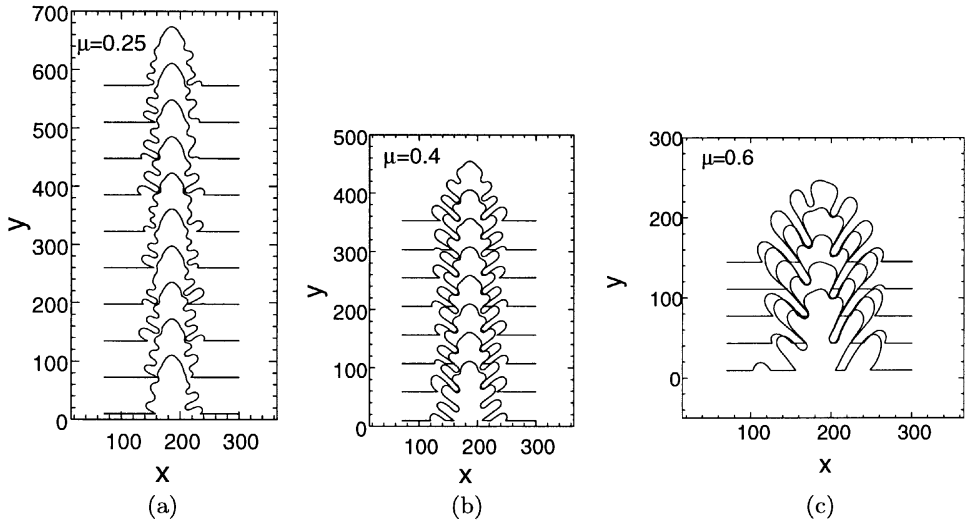

Fig. 3. Temporal evolution of a capillary dendrite for different values of μ. (a) $\mu = 0.25$, considerably below the critical value. (b) $\mu = 0.4$, and (c) $\mu = 0.6$, very close to the critical value. Parameters: $d_0 = 0.0417$, $\Delta = 0.5$, $\beta_0 = 1.5485$, $D = 1$, $\varepsilon_S = \varepsilon_K = 0.15$, $\theta_0 = \pi/4$. As before all length scales are given in internal units of the diffusional grid δx, all time scales are given in units of $\delta x^2/D$.

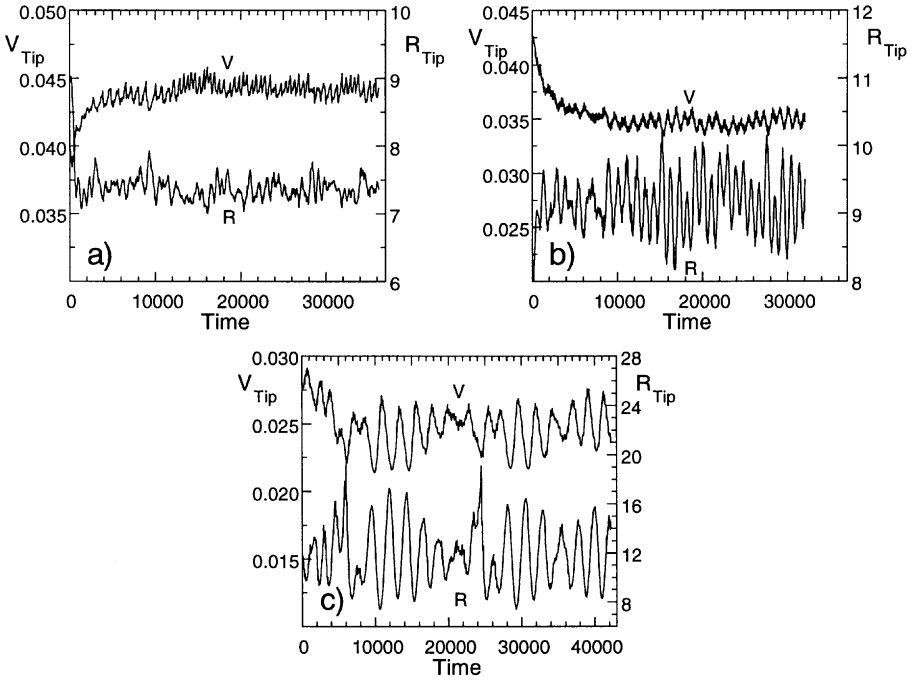

Fig. 4. The tip velocity V_{Tip} and the tip radius R_{Tip} for the capillary dendrites shown in Figure 3 are plotted *versus* time. a) $\mu = 0.25$, b) $\mu = 0.4$, and c) $\mu = 0.6$.

slower. These results are fully consistent with those Liu *et al.* [12] obtained in the boundary-layer approximation. From their work, which was also done at $\nu = 1$, a critical value of $\mu_{\mathrm{crit}} = 0.585$ can be extracted, which is very close to the value found here. Further investigations at a larger ratio of anisotropies, $\nu = 3.33$ ($\Delta = 0.5$, $\varepsilon_S = 0.075$, $\varepsilon_K = 0.25$) yielded $\mu_{\mathrm{crit}} = 0.135 \pm 0.003$. This is consistent with the predicted scaling $\mu_{\mathrm{crit}} \sim \nu^{-1}$, because based on the simulations at $\nu = 1$ the expected value would be $\mu_{\mathrm{theo}} = 0.617/\nu = 0.185$.

In summary, it was shown how a previously developed front-tracking method for dendritic growth can be generalized to incorporate kinetic effects. This was done by introducing an artificial dynamics at the phase boundary which does not influence the pattern formation. It was shown analytically how the time scale of this dynamics

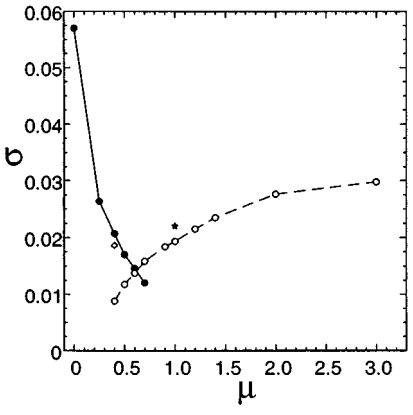

Fig. 5. The dimensionless growth rate $\sigma = V_{\rm Tip} d_0/(2Dp(\Delta)^2)$ is plotted *versus* μ at constant undercooling $\Delta = 0.5$ and anisotropy $\varepsilon_{\rm S} = \varepsilon_{\rm K} = 0.15$, $\theta_0 = \pi/4$. (•): capillary dendrite with $d_0 = 0.04166$; (◇): capillary dendrite, where all length scales (in units of the diffusional grid) were decreased by a factor of 1.6 to check the accuracy of the simulation; (○): kinetic dendrite with $d_0 = 0.04166/1.6$; (⋆): kinetic dendrite, where all length scales were increased by a factor of 1.6.

must be chosen to avoid numerical instabilities. The method was used to numerically study dendritic growth under the combined effect of surface tension anisotropy and an anisotropic kinetic coefficient. This can lead to oscillating dendrite-like structures which could not be investigated with previous quasi-stationary Green's function approaches. The results agree well with previous numerical work and are consistent with theoretical predictions. Both fundamental sidebranching mechanisms proposed in the literature, the selective amplification of noise at the tip of the dendrite and a non-linear mode of periodic tip deformations leading to correlated sidebranches on opposite sides of the dendrite, were observed. The first mechanism dominates far from the transition point, where dendrites change direction; the latter is important near the transition.

This study was performed at the Institut für Festkörperforschung, Forschungszentrum Jülich, Germany. I would like to thank H. Müller-Krumbhaar for support and many valuable discussions. I also thank D.M. Kroll for the critical reading of the manuscript. Support from the National Science Foundation under Grant No. DMR-9712134 and the donors of The Petroleum Research Fund, administered by the ACS, is gratefully acknowledged.

References

1. For reviews see: J.S. Langer, Rev. Mod. Phys. **52**, 1 (1980); *Lectures in the Theory of Pattern Formation in Chance and Matter, Les Houches 1986*, edited by J. Souletie *et al.* (Elsevier, Amsterdam, 1987); H. Müller-Krumbhaar, W. Kurz, *Phase Transformation in Materials*, edited by P. Haasen (VCH, Weinheim, 1991).
2. T. Ihle, H. Müller-Krumbhaar, Phys. Rev. Lett. **70**, 3083 (1993); Phys. Rev. E **49**, 2972 (1994); T. Ihle, diploma thesis, Universität Leipzig, Germany, 1992.
3. E. Brener, T. Ihle, H. Müller-Krumbhaar, Y. Saito, K. Shiraishi, Physica A **204**, 96 (1994).
4. S. Akamatsu, T. Ihle, Phys. Rev. E **56** 4479 (1997).
5. O. Pierre-Louis, C. Misbah, Phys. Rev. Lett. **76**, (1996) 4761; T. Ihle, C. Misbah, O. Pierre-Louis, Phys. Rev. B **58**, 2289 (1998).
6. W.K. Burton, N. Carbrera, F.C. Frank, Philos. Trans. R. Soc. London, Ser. A **243**, 299 (1951).
7. D. Kessler, J. Koplik, H. Levine, Phys. Rev. A **30**, 3161 (1984); **31**, 1712 (1985); **34**, 4980 (1986); Adv. Phys. **37**, 255 (1988).
8. A. Barbieri, D.C. Hong, J.S. Langer, Phys. Rev. A **35**, 1802 (1987).
9. M. Ben Amar, Y. Pomeau, Europhys. Lett. **2**, 307 (1986).
10. E.A. Brener, V.I. Mel'nikov, Adv. Phys. **40**, 53 (1991).
11. Y. Saito, T. Sakiyama, J. Crystal Growth **128**, 224 (1993), Note, that the scale of $\ln\lambda$ in Figure 1b is wrong. Correction: 1.0, 0.5, 0.0, −0.5 and −1.0 from top to bottom, Y. Saito (private communication).
12. F. Liu, N. Goldenfeld, Phys. Rev. A **42**, 895 (1990).
13. H. Emmerich, C. Misbah, K. Kassner, T. Ihle, J. Phys. Condens. Matter **11**, 9985 (1999).
14. G.P. Ivantsov, Dokl. Akad. Nauk. SSSR **58**, 567 (1947).
15. D.A. Kessler, H. Levine, Phys. Rev. Lett. **57**, 3069 (1986).
16. Y. Saito, G. Goldbeck-Wood, H. Müller-Krumbhaar, Phys. Rev. Lett. **58**, 1541 (1987); Phys. Rev. A **38**, 2148 (1988).
17. J.S. Langer, D.C. Hong, Phys. Rev. A **34**, 1462 (1986).
18. J.S. Langer, Phys. Rev. A **36**, 3350 (1987).
19. E. Brener, D. Temkin, Phys. Rev. E **51**, 351 (1995).
20. U. Bisang, J.H. Bilgram, Phys. Rev. E **54**, 5309 (1996).
21. A. Karma, W.-J. Rappel, Phys. Rev. E **60**, 3614 (1999).
22. O. Martin, N. Goldenfeld, Phys. Rev. A **36**, 1382 (1987).
23. M. Georgelin, A. Pocheau, Phys. Rev. E **57**, 3189 (1998).
24. T. Börzsönyi, T. Toth-Katona, A. Buka, L. Granasy, Phys. Rev. Lett. **83**, 2853 (1999).
25. X. Qian, H.Z. Cummings, Phys. Rev. Lett. **64**, 3038 (1990); B.T. Murray, A.A. Wheeler, M.E. Glicksman, J. Cryst. Growth **154**, 386 (1995).
26. Ph. Bouissou, A. Chiffaudel, B. Perrin, P. Tabeling, Europhys. Lett. **13**, 89 (1990).
27. H. Emmerich, D. Schleussner, T. Ihle, K. Kassner, J. Phys. Condens. Matter **11**, 8981 (1999).